
NUMERICAL INVESTIGATION OF FILLET WELDS EFFECTS ON THE LOCAL BUCKLING OF BOX STEEL COLUMNS

Seyed Shaker Hashemi^{1*}, Mehdi Hemmat², Kabir Sadeghi³,
Mohammad Vaghefi¹ & Amin Masihzadeh⁴

¹Department of Civil Engineering, Persian Gulf University, Shahid Mahini Street, Bushehr, Iran.

²University of Newcastle, School of Engineering, Newcastle, Australia.

³Department of Civil Engineering, Near East University, ZIP Code: 99138, Nicosia, North Cyprus, Mersin 10, Turkey.

⁴Department of Civil Engineering, Islamic Azad University of Bushehr, Varzesh Street, Bushehr, Iran.

*Corresponding author: sh.hashemi@pgu.ac.ir

Abstract: The local buckling has always been known as an undesirable and destructive phenomenon in steel structures. Thus, it is necessary to identify the effective factors in local buckling of the steel box column. Currently, box columns are generally fabricated by welding plates using fillet or groove welds with various manufacturing patterns, in terms of weld leg size and the overlap length of the plates. Hence, the evaluation of these patterns and also the control of local buckling in built sections seem to be essential. In this research, a variety of columns with different welding patterns, including groove and fillet welds with various overlap values and weld legs are numerically modeled and their local buckling behavior is studied in the finite element domain by using ABAQUS software. A suitable welding pattern is proposed by assessing the energy absorption, as well as stress distribution, stress concentration and finally local buckling in steel box section columns. The obtained results indicate that, the sections fabricated utilizing groove welds, have the best nonlinear performance. And also a suitable implementation of fillet welds to fabricate steel box columns is to consider 20% overlap length and 80% weld leg size to plate thickness as this model subject to small amount of local buckling. This model has shown less than 6% reduction in plastic capacity and energy absorption in comparison with groove welding. Another method is to use 50% for both overlap length and weld leg size to plate thickness. This model has shown less than 8% reduction in plastic capacity and energy absorption in comparison with groove welding. In addition, unsuitable implementation of fillet welds especially with small overlaps and weld leg sizes has shown a 12.5% reduction in plastic capacity and energy absorption, compared to groove welding

Keywords: Box steel column, groove weld, fillet weld, local buckling, weld leg size, overlap length, energy absorption

1.0 Introduction

Hollow sections have widely been used as suitable sections for the structural elements. They particularly have an advantageous effect on decreasing the mass of the structure due to their shapes. They are also used in other cases based on their geometrical features. Hollow sections are useful to endure against earthquake loads because of their high bending capacity. Moreover, they have higher gyration radius and accordingly are more economical in comparison with their equiponderant sections. Nowadays, these sections are assembled by plane plates. These plates are welded to each other by groove or fillet welds. The details of forming the box section made of plates and different welding methods are shown in Figure1. While the most feasible welding pattern for a groove weld is shown in Figure1, there are different patterns in terms of weld leg size and length of overlapping in a fillet weld, which are applied in fabricating box columns. Each of them can affect the local buckling behavior of box columns. Despite the numerous number of researches in the field of local buckling of box sections, there is still the lack of knowledge about the effects of weld leg size and overlap length of the plates on the local buckling behavior in box columns. Therefore, further studies are needed to detect the appropriate ratio between the weld leg size of fillet welds and the overlap length of the plates and to reduce the risk of local buckling in box columns.

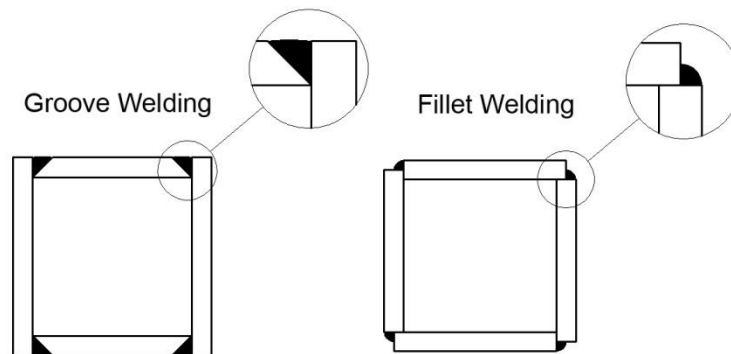


Figure1: Details of formation box section through groove and fillet welds

Many researchers have studied the local buckling of different steel shapes. They have considered the local buckling as an important part of the design process of structural steel, having different shapes. Some researchers have employed the theoretical approaches for local buckling simulation (Cuong 2013, Shen 2012, 2014, 2015) and some others have worked on the behavior and specifications of local buckling. Ostapenko (1977) investigated the local buckling of welded tubular columns by laboratory tests. Usami and Fukumoto (1982), Chiew *et al.* (1987) studied local and overall buckling of welded box columns by laboratory tests and derived a method to design such columns. Mulligan and Pekoz (1984) analyzed the locally buckled thin-

walled columns. Richard *et al.* (1988) performed numerical investigations of ultimate strength of thin-walled steel columns and finally provided an effective width for local buckling formula. Migita and Fukumoto (1997) studied the elasto-plastic behavior of local buckling in steel thin walled polygon sections numerically and experimentally. Uy (1998) investigated local and post-local buckling of concrete filled steel welded box columns and then studied the impacts of buckling on this section and derived the slenderness limits, and compared with the existing Australian and British standards. Uy (2000) studied slenderness and local buckling of plates in concrete filled steel box columns under compression and bending moment. Povlocic *et al.* (2010) performed laboratory tests to research the local buckling behavior of slender thin-walled box columns subjected to compression and bending. Seif and Schafer (2010) presented analytical expressions for the elastic local buckling stresses of hot-rolled steel structural profiles.

Wang *et al.* (2014) studied the behavior of axially compressed high strength steel box columns numerically and experimentally. Shen (2012, 2014) studied the ultimate strength of welded box section columns made of slender plate elements with large width to thickness ratios, ranging from 35 to 70 using the finite element analysis method. Moradi and Arwade (2014) used steel foams with high strength to weight ratio to fill the steel tubes to beneficially modify the response of steel tubes. They showed that steel foam improves significantly the ultimate strength and the capability of energy absorption of the steel tubes. They also illustrated that, if the composite action between steel foam and steel increases, the strength of the element will improve such a way that, the failure mode changes from local buckling to yielding.

Yang *et al.* (2016) studied the flexural buckling behavior of welded-section steel columns. The result of their research showed that the current design methods predict the buckling resistance of welded stainless steel box-section generally conservative. Thus, improvement could be anticipated. Hashemi *et al.* (2016) compared the capacity and energy absorption of box steel columns, fabricated with groove and fillet welds. Their obtained results indicate that the sections fabricated using groove welds have the best nonlinear performance and the sections with overlap size and weld leg equal to 20% and 80%, or 50% and 50% of plate thickness, respectively, lead to suitable performance. In addition, ANSI/AISC 360-10 (2010) and the Iranian national steel structural building code (2012) have provided overviews on the process of manufacturing and welding of steel box columns with plates as well as some requirements on the width to thickness ratios, to control the compact, non-compact and slender zones.

Despite the fact that, the buckling behavior of steel material is studied in the aforementioned researches, a closer look is missing to the effective factors of local buckling in the welded box columns. Therefore, in this research, a number of box columns, using the groove and fillet welding methods, with different weld leg size and overlapping length of the plates, are modeled numerically, employing the ABAQUS

finite element software, version 6.10.1 (2012). Finally, the local buckling behaviors of these models are investigated and based on the obtained results from analyses, the appropriate patterns of welding the steel box columns in terms of weld leg size and suitable overlapping length of the plates, are proposed.

2.0 Numerical Modeling

In this research, the ABAQUS finite element software with 8 –node cubic elements, has been employed for numerical modeling of the behavior of the examined samples. The examined samples are columns with the height of 2000 mm and cross-sectional dimensions of 200 mm×200 mm, which are made of plates with thicknesses of 10, 15 and 20 mm. An additional rigid plate is used at the top of columns, to prevent the stress concentration when applying the axial force. As a limitation in modeling, weld is not modeled separately because the material of plate and weld is identical in the process of modeling. So, as illustrated in Figure 2(a), the interaction effect is considered in the models, together with the fillet welds in the zones in which, the plates are in contact with each other without welding. This interaction is considered in modeling using stiff contact and without friction type (ABAQUS manual 2012).

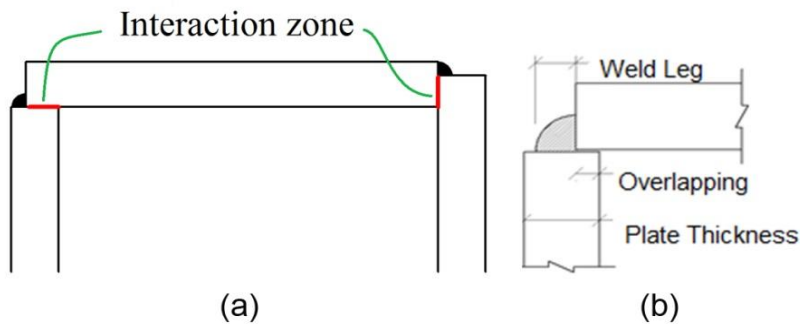


Figure 2: (a) Interaction zones; (b) Weld leg, overlapping and plate thickness in connecting zone

In the models with groove weld, the position of plates is fixed and the geometry is exactly similar to what's shown in Figure 1. But, in the models with fillet welds, it is feasible to change the behavior of samples by changing the overlap values of plates and also the weld leg size. Subsequently, the effects of these changes on the local buckling behavior of the samples are investigated. The meaning of weld leg, overlapping and plate thickness in a connecting zone of two welded plates is shown in Figure 2(b).

In this research, 18 and 3 samples with different geometry are made using fillet and groove welds, respectively. They have been investigated under 3 different axial and lateral loading patterns. In overall, 63 analyses have been performed. The names of the samples, initiate with

(a) or (g) which indicate the fillet and groove welds, respectively. A number is written just after the letters that indicates the thickness in millimeters of the plate used in the model. The second number is written with the letters (t) or (c), unless it is actually zero, represent the constant axial load on the model base, on a percentage of column's yielding strength. The letters (c) and (t) indicate compressive and tensile loads, respectively. The third and fourth numbers that are just written for a specimen with fillet weld, indicate the plate's overlapping size and weld leg size, both in millimeter. As an example, the g20-20t indicates that groove weld is used, the thickness of the plate is 20 mm and also a constant tensile axial load equal to 20% of the yield load of the column is exerted on the column under lateral load, during the nonlinear analyses. As another example, a15-0-3-4.5 indicates: fillet weld, the plates of 15 mm thickness, the applied axial load are zero, the overlapping of plates and the weld leg size are 3 mm and 4.5 mm, respectively. The details of models investigated in this research, are listed in table1. Given the amount of axial load, X can be one of 0, 20t, 40t, 20c, 40c and 60c quantities. St 37 steel is used in this research and the weld strengths are conservatively considered the same as those of steel. Moreover, as shown in Figure3, simplified stress-strain curve has been applied in this research to model the steel behavior. Modulus of elasticity and Poisson's ratio are considered 206010 MPa and 0.3, respectively, and the hardening model is assumed kinematic as default.

Table1: Detail of models

Name of models	Weld type	Plate thickness(mm)	Overlapping of plate(mm)	Weld leg size(mm)
a10-X-2-3	fillet	10	2	3
a10-X-2-5	fillet	10	2	5
a10-X-2-8	fillet	10	2	8
a10-X-5-3	fillet	10	5	3
a10-X-5-5	fillet	10	5	5
a10-X-7-3	fillet	10	7	3
g10-X	groove	10	-	-
a15-X-3-7.5	fillet	15	3	7.5
a15-X-3-12	fillet	15	3	12
a15-X-7.5-4.5	fillet	15	7.5	4.5
a15-X-7.5-7.5	fillet	15	7.5	7.5
a15-X-10.5-4.5	fillet	15	10.5	4.5
g15-X	groove	15	-	-
a20-X-4-6	fillet	20	4	6
a20-X-4-10	fillet	20	4	10
a20-X-4-16	fillet	20	4	16
a20-X-10-6	fillet	20	10	6
20-X-10-10	fillet	20	10	10
a20-X-14-6	fillet	20	14	6
g20-X	groove	20	-	-

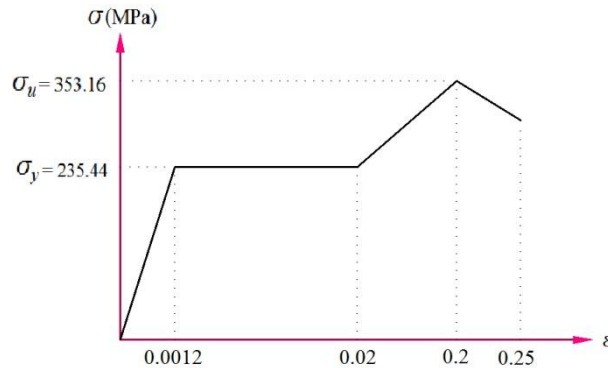


Figure 3: Applied stress-strain curve for steel

All models in this research are subject to six cases of load combinations. As shown in Figure 4, a lateral load is applied at top of the column while an axial constant load is exerted. The lateral load-displacement curve is investigated. The stress is evaluated using Von -Mises criteria in the most critical section at the column base. The applied constant axial loads on the models are as follows: $-0.6P_y$, $-0.4P_y$, $-0.2P_y$, $0P_y$, $+0.2P_y$, $+0.4P_y$. Where, P_y represents the yield axial load of the column ($P_y = A \times \sigma_y$). A , represents the cross section area of the column and σ_y , represents the yield stress of steel. Positive and negative signs show the tensile and compressive axial load, respectively. The data and information, used in the numerical method and also in the verification of the results, are based on the research of Hashemi *et al.* (2016). Besides, the validation of results is justified by comparing to the plastic bending capacity of sections derived by the theoretical method (Hashemi *et al.* 2016).

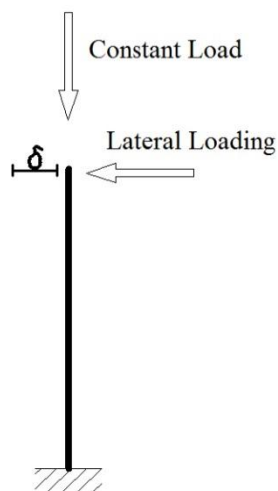


Figure 4: Loading condition of models

3.0 Research of Models Subjected to Different Loading Patterns

In this Section, the results of the analyses are compared with each other. Furthermore, the advantages and disadvantages of all models have been investigated, and the lateral load-displacement curves are plotted and assessed for all models. More researches were performed in the critical sections of column, whereas, local buckling and plastic hinges are more likely to occur in all analyzed models. The plastic bending moment (the ultimate bending strength) and the energy absorption (the area under the load-displacement curve) for each model are resulted from interpretation of these curves. Figures 5-7, show the load-displacement curves for columns fabricated with 10, 15 and 20 mm plates, respectively which are under axial compressive load equal to 40 percent of the yield strength (P_y).

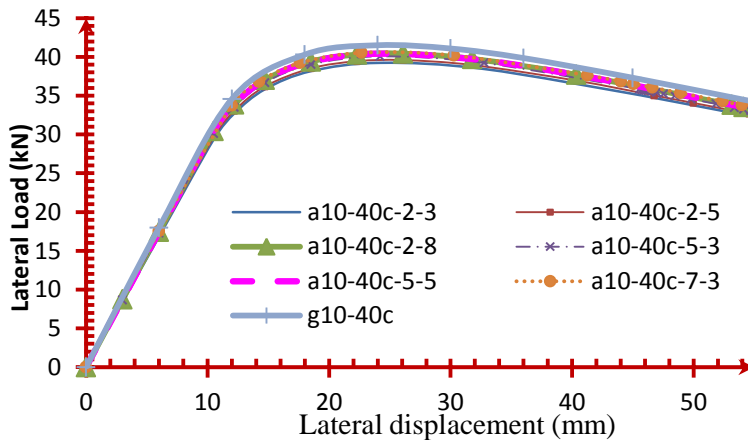


Figure 5: Lateral load- lateral displacement curves for columns fabricated with 10 mm plates under compressive axial load of $0.4P_y$

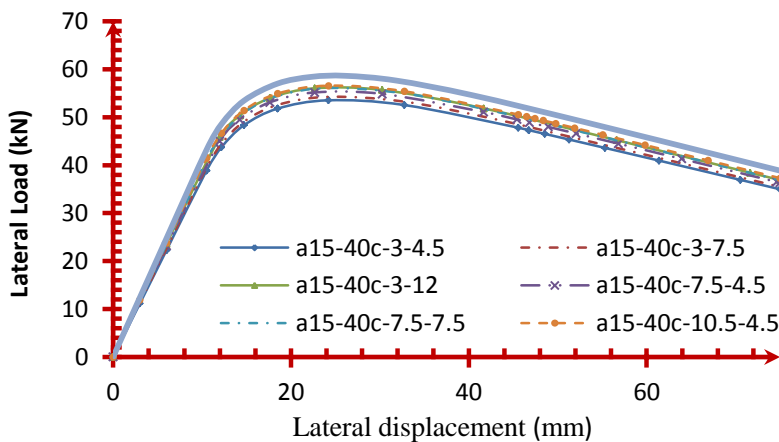


Figure 6: Lateral load- lateral displacement curves for columns fabricated with 15 mm plates under compressive axial load of $0.4P_y$

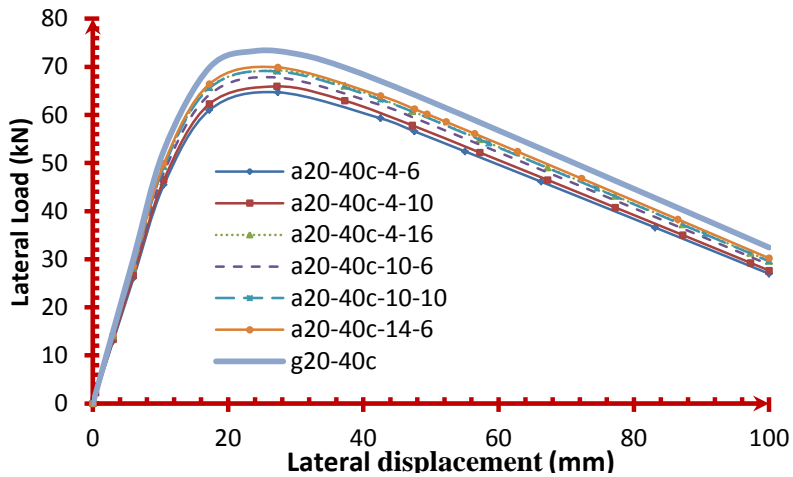


Figure 7: Lateral load-lateral displacement curves for columns fabricated with 20 mm plates under compressive axial load of $0.4P_y$

As shown in Figures 5-7, the model with groove weld shows the highest values, which means that, this model has the maximum energy absorption, maximum ductility and maximum strength among the columns examined with different geometry and assembly. It can be concluded, the column with groove weld is the best model for box sections. Table 2, presents the results obtained from nonlinear analyses on all models formed by plates with thickness of 10 mm and different welding characteristics subjected to different axial loads. The results, illustrate the reduction of the plastic capacity and the reduction of energy absorption per various axial loads compared to the optimum situation of groove weld and also the amount of local buckling in sides 1 and 4 of the models (Figure 8). The results of the similar process for the models formed by plates with the thickness of 15 and 20 mm have mentioned in Tables 3-4, respectively.

Table 2: Results of the models fabricated with 10 mm thickness plates subjected to various loading patterns

Model name	Overlap length to plate thickness ratio	Weld leg size to plate thickness ratio	Value of local buckling in critical section (Δ) (mm)		Percentage of reduction in plastic moment (%)
			Side 1	Side 4	
g10-0	--	--	9.89	1.97	--
a10-0-2-3	0.2	0.3	13.25	1.48	7.6
a10-0-2-5	0.2	0.5	11.45	1.47	6.7
a10-0-2-8	0.2	0.8	9.69	1.51	3.7
a10-0-5-3	0.5	0.3	12.27	1.56	4.7
a10-0-5-5	0.5	0.5	10.64	1.61	4.2
a10-0-7-3	0.7	0.3	12.27	1.61	2.7
g10-20c	--	--	10.84	2.25	--
a10-20c-2-3	0.2	0.3	16.74	1.95	5.7
a10-20c-2-5	0.2	0.5	13.48	1.97	4.8
a10-20c-2-8	0.2	0.8	8.62	2.00	2.6
a10-20c-5-3	0.5	0.3	14.81	2.09	3.5
a10-20c-5-5	0.5	0.5	11.70	2.09	2.7
a10-20c-7-3	0.7	0.3	12.3	2.07	2.1
g10-40c	--	--	10.84	2.25	--
a10-40c-2-3	0.2	0.3	0.1	0.3	0
a10-40c-2-5	0.2	0.5	0.66	0.47	5.5
a10-40c-2-8	0.2	0.8	0.34	0.26	4.6
a10-40c-5-3	0.5	0.3	0.14	0.23	2.6
a10-40c-5-5	0.5	0.5	0.36	0.24	3.5
a10-40c-7-3	0.7	0.3	0.19	0.24	2.6
g10-60c	--	--	0.04	0.13	--
a10-60c-2-3	0.2	0.3	0.22	0.10	6.1
a10-60c-2-5	0.2	0.5	0.09	0.09	5.9
a10-60c-2-8	0.2	0.8	0.06	0.10	4.2
a10-60c-5-3	0.5	0.3	0.13	0.10	5.1
a10-60c-5-5	0.5	0.5	0.07	0.12	4.2
a10-60c-7-3	0.7	0.3	0.07	0.10	3.8
g10-20t	--	--	6.58	1.38	--
a10-20t-2-3	0.2	0.3	9.01	0.87	5.9
a10-20t-2-5	0.2	0.5	7.97	0.89	5.2
a10-20t-2-8	0.2	0.8	6.79	0.96	2.5
a10-20t-5-3	0.5	0.3	8.26	0.95	3.6
a10-20t-5-5	0.5	0.5	7.27	0.96	2.6
a10-20t-7-3	0.7	0.3	7.64	1.00	2.2
g10-40t	--	--	3.34	1.00	--
a10-40t-2-3	0.2	0.3	4.30	0.42	4.6
a10-40t-2-5	0.2	0.5	3.84	0.47	3.8
a10-40t-2-8	0.2	0.8	3.37	0.58	2
a10-40t-5-3	0.5	0.3	4.64	0.60	3
a10-40t-5-5	0.5	0.5	4.11	0.60	2.3
a10-40t-7-3	0.7	0.3	3.43	0.56	1.6

Table 3: Results of the models fabricated with 15 mm thickness plates subjected to various loading patterns

Model name	Overlap length to plate thickness ratio	Weld leg size to plate thickness ratio	Value of local buckling in critical section (Δ) (mm)		Percentage of reduction in plastic moment (%)
			Side1	Side4	
g15-0	--	--	0.4	1.68	--
a15-0-3-4.5	0.2	0.3	2.74	0.78	12.6
a15-0-3-7.5	0.2	0.5	1.23	1.14	9.7
a15-0-3-12	0.2	0.8	0.56	1.20	4.8
a15-0-7.5-4.5	0.5	0.3	1.82	1.33	8
a15-0-7.5-7.5	0.5	0.5	1.07	1.32	5.8
a15-0-10.5-4.5	0.7	0.3	1.29	1.32	5.8
g15-20c	--	--	0.15	1.64	--
a15-20c-3-4.5	0.2	0.3	1.83	1.25	8.7
a15-20c-3-7.5	0.2	0.5	0.89	1.22	7.3
a15-20c-3-12	0.2	0.8	0.29	1.25	3.9
a15-20c-7.5-4.5	0.5	0.3	1.1	1.33	5.7
a15-20c-7.5-7.5	0.5	0.5	0.55	1.31	4
a15-20c-10.5-4.5	0.7	0.3	0.72	1.37	3.2
g15-40c	--	--	0.002	0.32	--
a15-40c -3-4.5	0.2	0.3	0.35	0.29	8.7
a15-40c -3-7.5	0.2	0.5	0.11	0.28	7.5
a15-40c -3-12	0.2	0.8	0.02	0.26	4.4
a15-40c -7.5-4.5	0.5	0.3	0.13	0.29	5.9
a15-40c -7.5-7.5	0.5	0.5	0.04	0.28	4.3
a15-40c -10.5-4.5	0.7	0.3	0.06	0.29	3.5
g15-60c	--	--	0.002	0.14	--
a15-60c -3-4.5	0.2	0.3	0.14	0.12	10
a15-60c -3-7.5	0.2	0.5	0.05	0.12	9
a15-60c -3-12	0.2	0.8	0.01	0.11	5.8
a15-60c -7.5-4.5	0.5	0.3	0.05	0.11	7.3
a15-60c -7.5-7.5	0.5	0.5	0.02	0.12	5.8
a15-60c -10.5-4.5	0.7	0.3	0.02	0.12	4
g15-20t	--	--	0.70	1.46	--
a15-20t-3-4.5	0.2	0.3	2.06	0.67	6.8
a15-20t-3-7.5	0.2	0.5	1.34	0.76	5.8
a15-20t-3-12	0.2	0.8	0.87	0.89	3
a15-20t-7.5-4.5	0.5	0.3	1.64	0.77	4.2
a15-20t-7.5-7.5	0.5	0.5	1.18	0.85	3
a15-20t-10.5-4.5	0.7	0.3	1.44	0.82	2.5
g15-40t	--	--	0.72	1.11	--
a15-40t-3-4.5	0.2	0.3	1.12	0.21	6.8
a15-40t-3-7.5	0.2	0.5	0.94	0.35	5.8
a15-40t-3-12	0.2	0.8	0.83	0.23	3
a15-40t-7.5-4.5	0.5	0.3	1.02	0.29	4.2
a15-40t-7.5-7.5	0.5	0.5	0.94	0.42	3
a15-40t-10.5-4.5	0.7	0.3	0.97	0.36	2.5

Table 4: Results of the models fabricated with 20 mm thickness plates subjected to various loading patterns

Model name	Overlap length to plate thickness ratio	Weld leg size to plate thickness ratio	Value of local buckling in critical section (Δ) (mm)		Percentage of reduction in plastic moment (%)
			Side1	Side4	
g20-0	--	--	0.72	1.71	--
a20-0-4-6	0.2	0.3	0.43	0.73	12.5
a20-0-4-10	0.2	0.5	0.20	0.81	10.4
a20-0-4-16	0.2	0.8	0.06	1.00	5.4
a20-0-10-6	0.5	0.3	0.27	0.97	7.8
a20-0-10-10	0.5	0.5	0.16	1.05	5.8
a20-0-14-6	0.7	0.3	0.27	0.65	4.7
g20-20c	--	--	0.72	1.39	--
a20-20c-4-6	0.2	0.3	0.41	0.90	12
a20-20c-4-10	0.2	0.5	0.13	0.90	10.1
a20-20c-4-16	0.2	0.8	0.02	0.92	5.3
a20-20c-10-6	0.5	0.3	0.20	0.98	7.4
a20-20c-10-10	0.5	0.5	0.09	0.98	5.6
a20-20c-14-6	0.7	0.3	0.13	1.03	4.3
g20-40c	--	--	0.45	0.37	--
a20-40c-4-6	0.2	0.3	0.17	0.31	11.7
a20-40c-4-10	0.2	0.5	0.04	0.30	10
a20-40c-4-16	0.2	0.8	0.18	0.27	5.6
a20-40c-10-6	0.5	0.3	0.05	0.32	7.6
a20-40c-10-10	0.5	0.5	0.01	0.31	5.8
a20-40c-14-6	0.7	0.3	0.03	0.34	4.6
g20-60c	--	--	0.12	0.10	--
a20-60c-4-6	0.2	0.3	0.04	0.08	13.7
a20-60c-4-10	0.2	0.5	0.007	0.08	11
a20-60c-4-16	0.2	0.8	0.001	0.07	7.4
a20-60c-10-6	0.5	0.3	0.008	0.08	9.4
a20-60c-10-10	0.5	0.5	0.002	0.08	7.7
a20-60c-14-6	0.7	0.3	0.005	0.08	6.4
g20-20t	--	--	0.08	1.46	--
a20-20t-4-6	0.2	0.3	0.33	0.52	10.2
a20-20t-4-10	0.2	0.5	0.20	0.62	9.4
a20-20t-4-16	0.2	0.8	0.12	0.76	4.5
a20-20t-10-6	0.5	0.3	0.29	0.61	6.3
a20-20t-10-10	0.5	0.5	0.21	0.70	4.7
a20-20t-14-6	0.7	0.3	0.26	0.66	3.7
g20-40t	--	--	0.15	1.23	--
a20-40t-4-6	0.2	0.3	0.18	0.19	9.2
a20-40t-4-10	0.2	0.5	0.15	0.31	7.8
a20-40t-4-16	0.2	0.8	0.16	0.52	4
a20-40t-10-6	0.5	0.3	0.19	0.23	5.7
a20-40t-10-10	0.5	0.5	0.19	0.36	4.2
a20-40t-14-6	0.7	0.3	0.20	0.27	3.3

As it is illustrated in Tables 2-4, in the fillet welded columns with 10 mm plates and with a short overlap length and a small weld leg size, significant reduction about 11.38% has been observed in the energy absorption, compared to groove welded models. This reduction was about 7.6% for plastic capacity. Similarly, the observed reduction in energy absorption for columns fabricated with 15 mm and 20 mm plates were 10.42% and 13.48%, respectively. The reductions in the plastic capacity in the former columns were about 12.6% and 13.7% in the same order. The load-displacement curves reveal that, by decreasing the thickness of conducted plates in fabricating columns, the identical behavior of columns is observed, although the manufacturing and assembly procedures are different. Conversely, by increasing the thickness of the plates, due to the amplification of total capacity, the dispersal between plastic capacities of the models, influenced by the method of manufacturing and assembly, is more significant.

Regarding the overlap length and weld leg size, more options are observed in the geometry and method of welding of the models with fillet weld. Furthermore, increasing the fillet weld size has resulted to increase the energy absorption and ductility of the models. But, defining the exact size of weld leg and the overlap length of plates leading to the optimal behavior of the column is not so obvious. Based on the obtained results from the analyzed models, to enhance the capacity, increasing the length of overlap of plates interferes more significantly than increasing the weld leg size. Among all the models examined with fillet weld, the model in which the length of overlap of plates is maximized and consequently the weld leg size is minimized has the maximum plastic capacity, energy absorption and ductility. In other words, their capacity has the least differences compared to the models with groove weld.

In the model having a large length overlap and a small weld leg size, the ratios of overlap length and weld leg size to the plate thickness are 0.7 and 0.3, respectively. As it can be observed from Figures 5-7, the curve of this model has the highest amount of energy absorption and plastic capacity following the model fabricated with groove welding. As a general conclusion, when the ratios of overlap and weld leg size to the plate thickness are 0.7 and 0.3, the column with fillet weld has the highest energy absorption, ductility and plastic capacity. Besides, the differences in energy absorption and plastic capacity compared to the groove welded models are less than 5% for 10 mm plate models and 5.8 and 4.1 for cases with 15 mm plate, respectively. These analyses for the models with 20 mm plate illustrate the maximum of 6.4% and 5.98% of reduction in energy absorption and plastic capacity compared to groove welded models. Besides, the energy absorption, ultimate strength, local buckling behavior has been investigated at the most critical section at the column base, where, the local buckling and plastic hinges are most likely to occur. In order to better understand the process of evaluating the local buckling of plates in the columns, different sides of the column are numbered with numbers 1 to 4 (Figure8).

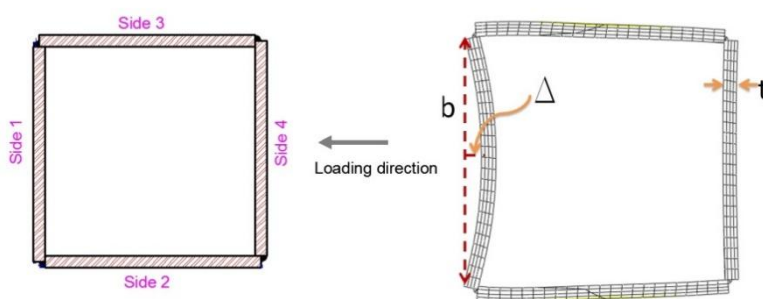


Figure 8: Nomenclature of different sides of square section and monitored value for local buckling

The evaluation of the samples indicates that, the maximum amount of local buckling is observed in the column fabricated with 10 mm plate ($b/t \geq 20$) and this amount decreased in column made by 15 mm plate. Finally, in the cases of the box columns with 20 mm plates, the least amount of local buckling is observed. This is due to the effect of the reduction in width to thickness ratio and the increase in compaction on the samples. In other words, the effect of local buckling is considerable for box columns with 10 mm plates and $b/t = 20$. This effect decreases for columns with $b/t \leq 20$ as far as in the columns with the ratio of $b/t \leq 10$, the local buckling effect is not observed in their nonlinear behavior. Nonetheless, the local buckling is negligible for box columns made with 15mm and 20 mm plates; they are investigated regardless of the local buckling effects in this research. This is in order to research the effects of weld leg size and plate overlap length on the capacity and energy absorption. Moreover, the studies of columns, fabricated with fillet welds, show that, the amount of local buckling decreases with increasing the weld leg size.

As an example, for a 200 mm displacement at the top of the column in models a10-0-2-3, a10-0-2-5 and a10-0-2-8, the local buckling in side 1 are 13.25 mm, 11.45mm and 9.69mm, respectively. Figure 9 shows a critical section of the column in which the local buckling is observed. The effect of an increase in the weld leg size on the reduction of the local buckling amount is graphically perceptible. As it can be observed in Tables 2 to 4 and Figure 10, the increase in the compressive axial load up to 20% of P_y on the models with constant lateral displacement leads to increase the local buckling. For example, the local buckling in the models a10-0-2-3 and a10-20c-2-3 are 13.25mm and 16.74mm, respectively. To better explain, the presence of axial load up to 20% of P_y , shifts the failure mechanism from pure bending to interaction between bending moment and axial force, and reduces the local buckling that is more affected by flexural buckling.

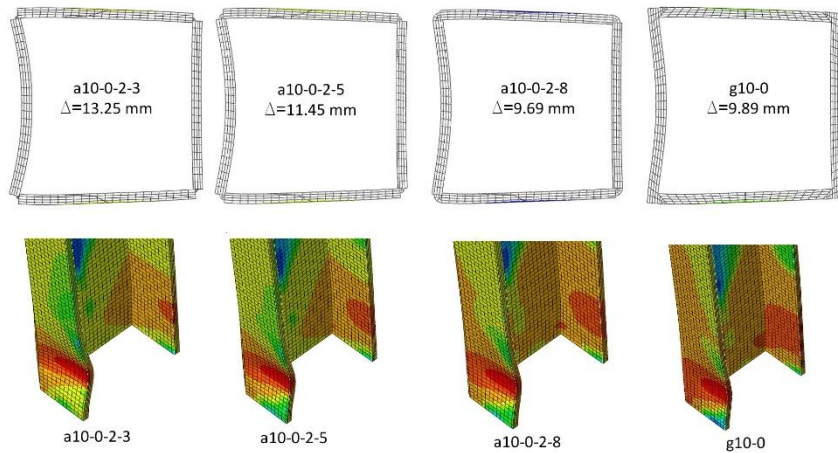


Figure 9: The reduction of local buckling due to the increase in the fillet weld leg size (a10-0 models)

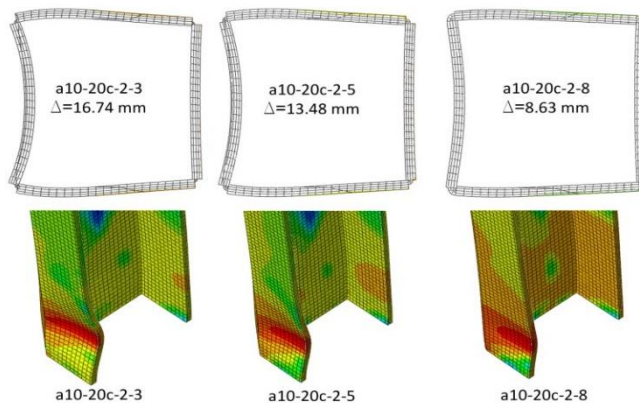


Figure10: The reduction of local buckling due to the increase in the fillet weld leg size (a10-20c models)

Furthermore, the analyses indicate that the increase in the overlap length of the plates can result the reduction of local buckling. For instance, in Figure11, for a 200 mm displacement applied at the top of the column in models a10-20c-2-3, a10-20c-5-3 and a10-20c-7-3, the resulted local buckling in side 1 are 16.74 mm, 14.81mm and 12.3mm, respectively. The investigations on the models with fillet welds reveal that, the increase of weld leg size is more effective than the increase in the overlap length of the plates in decreasing the local buckling in box columns. Based on Table 2, the local buckling of side 1 in Sample a10-20-2-3 is 16.74 mm. On the one hand, the local buckling in this side is decreased approximately to half (8.62 mm) by adding 5 mm to weld leg size. On

the other hand, this decreases to three quarters of the initial value (12.3 mm) by increasing 5 mm to the overlap length.

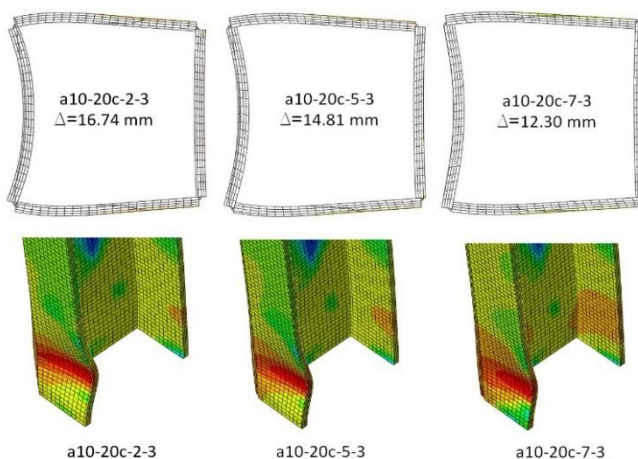


Figure11: The reduction of local buckling due to the increase in the overlap length of the plates (a10-20c models)

In addition to the side 1, local buckling occurs in other sides of models as well. Specially, the direct relation between weld leg size and overlap length of plates with local buckling in the side 4 is remarkable. Although the local buckling is not significant in side 4, this usually decreases with increasing the weld leg size and overlap length of the plates. In other words, the decline of local buckling in the side 1, brings enhancement of local buckling in the side 4 of the models. This can be observed in Tables 2 to 4. Figure12 shows the critical section of the column base, in different models and the changes in weld leg size values in constant overlap length. Although the results indicate the inconsequential amount of local buckling, this amount is decreased by increasing the weld leg size. The local buckling amount experiences a significant decline in weld leg size equal to 80% of the plate thickness. This amount of local buckling is very close to its equivalent values in the groove welded model.

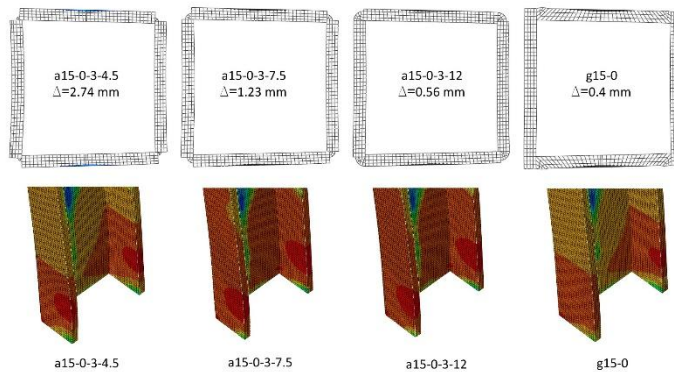


Figure12: The reduction of local buckling due to the increase in the fillet weld leg size (a15-0 models)

Evaluation of models fabricated with groove weld shows that, these models have small amounts of local buckling. The least amount of local buckling happened in the models fabricated with fillet weld in which the ratio of weld leg size and overlap length to the plate thickness are 0.8 and 0.2 or 0.5 and 0.5, respectively. The groove weld has maximum values of energy absorption and capacity in box columns. But due to the operational difficulties of groove weld, the fillet weld is widely used in fabricating steel box columns. Moreover, models fabricated with fillet welds in which the ratios of weld leg size and overlap length to the plate thickness are 0.3 and 0.7, are good in energy absorption and capacity, but inappropriate in the local buckling compared to the similar models in which the ratio of weld leg size and overlap length to the plate thickness are 0.8 and 0.2 or 0.5 and 0.5, respectively. Hence, a suitable implementation of fillet welds to fabricate steel box columns is to consider 20% overlap length and 80% weld leg size to plate thickness. This model has shown less than 6% reduction in plastic capacity and energy absorption compared to groove welding.

4.0 Conclusions

In this research, a variety of columns with different welding patterns, including groove and fillet welding with various overlap values and weld leg size are numerically modeled and their local buckling behavior is studied by using the finite element ABAQUS software. The results show:

- According to the investigations, groove weld has the best performance for the ductility and energy absorption in box columns. But, due to the operational difficulties of groove weld, the fillet weld is widely used in fabricating steel box columns.

- Among fillet welded models, the increase in the weld leg size and the overlap length of the plates can reduce the amount of local buckling in the box columns. However, the numerical modeling comparison between both of them, shows the more effectiveness due to increase in weld leg size.
- In the models with larger overlap lengths and smaller weld leg sizes, the energy absorption and plastic capacity are considerably improved. But, they are not the most suitable alternative for groove welded models because of inappropriate local buckling behavior in these columns compared to the models in which the ratios of weld leg size and overlap length to the plate thickness are 0.8 and 0.2 or 0.5 and 0.5, respectively. In overall, the differences in the examined models are not significant and they show good capacity in energy absorption, plastic moment (not the best ones) and also suitable behavior in terms of local buckling. For better explanation, a suitable implementation of fillet welds to fabricate steel box columns is to consider 20% overlap length and 80% weld leg size to plate thickness as this model subject to small amount of local buckling. This model has shown less than 6% reduction in plastic capacity and energy absorption in comparison with groove welding. Another method is to use 50% for both overlap length and weld leg size to plate thickness. This model has shown less than 8% reduction in plastic capacity and energy absorption in comparison with groove welding.
- Unsuitable implementation of fillet welds especially with small overlaps and weld leg sizes has shown a 12.5% reduction in plastic capacity and energy absorption, compared to groove welding. Small thickness may cause significant stress concentration in welds and local buckling in plates. This result, emphasis on accurate attention in providing proper overlap length and weld leg size in the process of fabricating steel box columns.

References

- ABAQUS Standard User's Manual, (2012), Version 6.10.1, New York, USA.
- ANSI/ASCE 360-10 (2010). Specification for Structural Steel Buildings. American Institute of Steel Construction, Chicago, IL.
- Chiew, S., Lee, S. and Shanmugam, N. (1987) Experimental research of thin-walled steel box column, *Structural Engineering*, 113(10): 2208-2220.
- Cuong, B. (2013) Buckling of thin-walled members analyzed by Mindlin-Reissner finite strip, *Structural Engineering and Mechanics*, 48 (1): 77-91.
- Hashemi, S., Vaghefi, M., Hemmat, M. and Masihzadeh, A, (2016) Comparison the capacity of box steel columns, fabricated with groove and fillet welds, *International Journal of Steel Structures*, 16(2): 373-382.
- Iranian National Steel Structural Building Code (2012), Design and Implementation of Steel Structures, Iran Department of Housing and Urban Development, Tehran, Iran.

- Migita, Y. and Fukumoto, Y. (1997) Local buckling behavior of polygonal sections, *Constructional Steel Research*, 41(2-3): 221-233.
- Moradi, M. and Arwade, S. (2014) Improving buckling response of the square steel tube by using steel foam, *Structural Engineering and Mechanics*, 51(6): 1017-1036.
- Mulligan, G.P. and Pekoz, T. (1984) Analysis of Locally Buckled Thin-Walled Columns, *Seventh International Specialty Conference on Cold-Formed Steel Structures*, St. Louis, Missouri, U.S.A.
- Ostapenko, A. (1977) Local buckling of welded tubular columns, *Thin-Walled Structures*, 40(2): 109-123.
- Povlocic, L., Froschmeier, B., Kuhlmann, U. and Beg, D. (2010) Slender thin-walled box columns subjected to compression and bending, *Journal of Civil Engineering and Management*, 16(2): 179-188.
- Richard Liew, J.Y., Shanmugam, N.E. and Lee, S.L. (1988) Local buckling of thin-walled steel box columns, *Thin-Walled Structures*, 8(2): 119-145.
- Seif, M. and Schafer, B.W. (2010) Local buckling of structural steel shapes, *Constructional Steel Research*, 66(10): 1232-1247.
- Wang, Y., Li, G., Chen, S., Sun, F. (2014) Experimental and numerical study on the behavior of axially compressed high strength steel box-columns, *Engineering Structures*, 58:79-91.
- Shen, H. (2012) Ultimate capacity of welded box section columns with slender plate elements, *Steel and Composite Structures*, 13(1): 15-33.
- Shen, H. (2014) On the direct strength and effective yield strength method design of medium and high strength steel welded square section columns with slender plate elements, *Steel and Composite Structures*, 17(4): 497-516.
- Shen, H. (2015), Behavior of high-strength steel welded rectangular section beam-columns with slender webs, *Thin-Walled Structures*, 88: 16-27.
- Usami, T. and Fukumoto, Y. (1982) Local and overall buckling of welded box columns, *Structural Division*, 108(3): 525-542.
- Uy, B. (1998), "Local and post-local buckling of concrete filled steel welded box columns, *Constructional Steel Research*, 47(1-3): 47-72.
- Uy, B. (2000) Strength of concrete filled steel box columns incorporating local buckling, *Structural Engineering*, 126(3): 341-352.
- Yang, L., Zhao, M., Xu, D., Shang, F., Yuan, H., Wange, Y. and Zhang, Y. (2016) Flexural buckling behavior of welded stainless steel box-section columns, *Thin-Walled Structures*, 104: 185-197.